



On the global synchronization of pulse-coupled oscillators interacting on chain and directed tree graphs[☆]

Huan Gao, Yongqiang Wang^{*}

Department of Electrical and Computer Engineering, Clemson University, Clemson, SC 29634, United States

ARTICLE INFO

Article history:

Received 28 January 2018

Received in revised form 25 October 2018

Accepted 6 February 2019

Available online 18 March 2019

Keywords:

Global synchronization
Pulse-coupled oscillators
Hybrid systems

ABSTRACT

Driven by increased applications in biological networks and wireless sensor networks, synchronization of pulse-coupled oscillators (PCOs) has gained increased popularity. However, most existing results address the *local* synchronization of PCOs with initial phases constrained in a half cycle, and results on *global* synchronization from *any initial condition* are very sparse. In this paper, we address *global* PCO synchronization from an arbitrary phase distribution under chain or directed tree graphs. Our results differ from existing global synchronization studies on decentralized PCO networks in two key aspects: first, our work allows heterogeneous coupling functions, and we analyze the behavior of oscillators with perturbations on their natural frequencies; second, rather than requiring a large enough coupling strength, our results hold under any coupling strength between zero and one, which is crucial because a large coupling strength has been shown to be detrimental to the robustness of PCO synchronization to disturbances.

© 2019 Elsevier Ltd. All rights reserved.

1. Introduction

Pulse-coupled oscillators (PCOs) are limit cycle oscillators coupled through exchanging pulses at discrete time instants. They were originally proposed to model the synchronization phenomena in biological systems, such as contracting cardiac cells, flashing fireflies, and firing neurons (Ermentrout, 1996; Mirollo & Strogatz, 1990; Peskin, 1975). Due to their amazing scalability, simplicity, and robustness, recently they have found applications in wireless sensor networks (Hong & Scaglione, 2005; Hu & Servetto, 2006; Pagliari & Scaglione, 2011; Simeone, Spagnolini, Bar-Ness, & Strogatz, 2008), image processing (Rhouma & Frigui, 2001), and motion coordination (Gao & Wang, 2018).

Early results on PCO synchronization were motivated by biological applications, and normally assume a fixed interaction or coupling mechanism (Mirollo & Strogatz, 1990; Peskin, 1975). In engineering applications, such restrictions do not exist any more. In fact, the interaction mechanism becomes a design variable that provides opportunities to achieve desired performance. For example, Mauroy (2011) and Nishimura and Friedman (2011) designed

the interaction to improve the robustness to communication delays. Our prior work (Wang & Doyle III, 2012) optimized the interaction, i.e., phase response function (PRF), to improve the speed of synchronization. However, most of these results are for local synchronization assuming that the initial phases are restricted within a half cycle (Achuthan & Canavier, 2009; Acker, Kopell, & White, 2003; Canavier & Achuthan, 2010; Dror, Canavier, Butera, Clark, & Byrne, 1999; Ermentrout, 1996; Ernst, Pawelzik, & Geisel, 1995; Goel & Ermentrout, 2002; Hansel, Mato, & Meunier, 1995; Kannapan & Bullo, 2016; Kirk & Stone, 1997; LaMar & Smith, 2010; Memmesheimer & Timme, 2010; Nishimura & Friedman, 2011; Proskurnikov & Cao, 2015, 2017; Timme & Wolf, 2008; Timme, Wolf, & Geisel, 2002; Vreeswijk, Abbott, & Ermentrout, 1994; Wang & Doyle III, 2012; Wang, Núñez, & Doyle III, 2012, 2013a).

Assuming restricted initial phase distribution severely hinders the application of PCO based synchronization, since in distributed systems it is hard to control the initial phase distribution. Recently, efforts have emerged to address global PCO synchronization from an arbitrary initial phase distribution. However, these results focus on special graphs, such as all-to-all graph (Canavier & Tikidji-Hamburyan, 2017; Klinglmayr & Bettstetter, 2012; Konishi & Kokame, 2008; Núñez et al., 2015a), cycle graph (Núñez et al., 2015b), strongly-rooted graph (Núñez et al., 2015a), or master/slave graph (Núñez et al., 2016). Moreover, they rely on sufficiently large coupling strengths, which may not be desirable as large coupling strengths are detrimental to robustness to disturbances (Hong & Scaglione, 2005).

[☆] The work was supported in part by the National Science Foundation, United States under Grant 1738902. The material in this paper was not presented at any conference. This paper was recommended for publication in revised form by Associate Editor Zhihua Qu under the direction of Editor Daniel Liberzon.

^{*} Corresponding author.

E-mail addresses: hgao2@clemson.edu (H. Gao), yongqi@w.clemson.edu (Y. Wang).

Table 1

Comparison of our results with other results.

		Homogeneous coupling		Heterogeneous coupling	
		PCO network having (at least) a global node ^a	Decentralized PCO networks	PCO network having (at least) a global node	Decentralized PCO networks
Non-global synchronization	Local synchronization	Achuthan and Canavier (2009), Acker et al. (2003), Canavier and Achuthan (2010), Ermentrout (1996), Ernst et al. (1995), Goel and Ermentrout (2002), Hansel et al. (1995), Kirk and Stone (1997), Konishi and Kokame (2008), Núñez, Wang, and Doyle III (2015a) and Vreeswijk et al. (1994)	Goel and Ermentrout (2002), Kannapan and Bullo (2016), LaMar and Smith (2010), Memmesheimer and Timme (2010), Nishimura and Friedman (2011), Núñez et al. (2015a), Núñez, Wang, and Doyle III (2015b), Proskurnikov and Cao (2015), Timme and Wolf (2008), Timme et al. (2002), Wang and Doyle III (2012) and Wang et al. (2012, 2013a)	Núñez, Wang, Teel, and Doyle III (2016)	Dror et al. (1999) and Proskurnikov and Cao (2017)
	Almost global synchronization or synchronization with probability one	Chen (1994), Mathar and Mattfeldt (1996) and Mirollo and Strogatz (1990)	Klinglmayr, Bettstetter, Timme, and Kirst (2017), Klinglmayr, Kirst, Bettstetter, and Timme (2012) and Lyu (2015)	\	\
Global synchronization	Discrete state synchronization	An, Zhu, Li, Xu, Xu, and Li (2011)	Lyu (2015)	\	\
	(Continuous) phase synchronization	Canavier and Tikidji-Hamburyan (2017), Klinglmayr and Bettstetter (2012), Konishi and Kokame (2008) and Núñez et al. (2015a)	Lyu (2018) ^b and Núñez et al. (2015a,b)	Núñez et al. (2016)	This paper

^aA node is called as a global node if it is directly connected to all the other nodes.^bNote that when the maximum degree of an undirected tree graph is not over 3, Lyu (2018) obtained global synchronization results for the conventional phase-only PCO model, though results were also obtained under general undirected tree graphs for a more complicated PCO model with multiple additional state variables.

In this paper, we address the global synchronization of PCOs under arbitrary initial conditions and heterogeneous coupling functions (PRFs). Our main focus is on the global synchronization of PCOs under undirected chain graphs, but the results are easily extendable to PCO synchronization under directed chain/tree graphs. Note that the chain or directed tree graphs are basic elements for constructing more complicated graphs and are desirable in engineering applications where reducing the number of connections is important to save energy consumption and cost in deployment/maintenance. Furthermore, the chain graph has been regarded as the worst-case scenario for synchronization due to its minimum number of connections (Klinglmayr & Bettstetter, 2010). We also consider oscillators with perturbations on their natural frequencies. Compared with existing results including our prior work (cf. Table 1), this paper has the following contributions: (1) Different from most existing results which focus on local PCO synchronization and assume that the initial phases of oscillators are restricted within a half cycle, our work addresses global synchronization from an arbitrary initial phase distribution; (2) Different from existing global synchronization studies on decentralized PCO networks, our work allows heterogeneous phase response functions, and we analyze the behavior of oscillators with perturbations on their natural frequencies. These scenarios, to our knowledge, have not been considered in any existing global synchronization results on decentralized PCO networks; (3) In contrast to existing global PCO synchronization results requiring a strong enough coupling strength, our results guarantee global synchronization under any coupling strength between zero and one, which is more desirable since a very strong coupling strength, although can bring fast convergence, has been shown to be detrimental to the robustness of synchronization to disturbances (Hong & Scaglione, 2005).

It is worth noting that even in the theoretical derivation point of view, this paper also differs significantly from our prior work (Núñez et al., 2015a,b, 2016): (1) Different from our prior

work (Núñez et al., 2015a,b, 2016) whose proofs are essentially based on local synchronization analysis, this work presents a direct global analyzing approach. More specifically, to obtain global synchronization results, our prior work (Núñez et al., 2015a,b, 2016) used **strong enough** coupling strengths to reduce the network to a state where all phases are contained in a half cycle, and then achieved global synchronization based on local synchronization analysis. In comparison, this work studies the systematic evolution of phases even when they are not restricted in a half cycle, and hence can allow the coupling strength to be any value between zero and one; (2) Although the Lyapunov candidate function seems similar to the one used in our prior work (Núñez et al., 2015b), the analysis here is much more complicated due to the considered more complicated scenarios (arbitrary coupling strength between zero and one and heterogeneous PRFs). In fact, to address synchronization under such scenarios, we had to introduce Invariance Principle, which is not needed in our prior results (Núñez et al., 2015a,b, 2016) due to their simple dynamics brought by strong and homogeneous coupling.

The outline of this paper is as follows. Section 2 introduces preliminary concepts. A hybrid model for PCO networks and its dynamical properties are presented in Section 3. In Section 4, we analyze global synchronization on both chain and directed tree graphs and provide robustness analysis under frequency perturbations. Numerical experiments are given in Section 5. Finally, we conclude the paper in Section 6.

2. Preliminaries

2.1. Basic notation

\mathbb{R} , $\mathbb{R}_{\geq 0}$, and $\mathbb{Z}_{\geq 0}$ denote real numbers, nonnegative real numbers, and nonnegative integers, respectively. \mathbb{R}^n denotes the Euclidean space of dimension n , and $\mathbb{R}^{n \times n}$ denotes the set of $n \times n$

square matrices with real coefficients. \mathbb{B} denotes the closed unit ball in the Euclidean norm. A set-valued map $M : A \rightrightarrows B$ associates an element $\alpha \in A$ with a set $M(\alpha) \subseteq B$; the graph of M is defined as $\text{graph}(M) := \{(\alpha, \beta) \in A \times B : \beta \in M(\alpha)\}$. M is outer-semicontinuous if and only if its graph is closed (Rockafellar & Wets, 2009). The range of a function $f : \mathbb{R}^n \rightarrow \mathbb{R}^m$ is denoted as $\text{rge} f$. The closure of set \mathcal{A} is denoted as $\bar{\mathcal{A}}$. The distance of a vector $x \in \mathbb{R}^n$ to a closed set $\mathcal{A} \subset \mathbb{R}^n$ is denoted as $|x|_{\mathcal{A}} = \inf_{y \in \mathcal{A}} |x - y|$. The μ -level set of function $V : \text{dom } V \rightarrow \mathbb{R}$ is denoted as $V^{-1}(\mu) = \{x \in \text{dom } V : V(x) = \mu\}$ (Goebel, Sanfelice, & Teel, 2012).

2.2. Hybrid systems

We use hybrid systems framework with state $x \in \mathbb{R}^n$ (Goebel et al., 2012)

$$\mathcal{H} : \begin{cases} \dot{x} = f(x), & x \in \mathcal{C} \\ x^+ \in G(x), & x \in \mathcal{D} \end{cases} \quad (1)$$

where f , \mathcal{C} , G , and \mathcal{D} are the flow map, flow set, jump map, and jump set, respectively. The hybrid system can be represented by $\mathcal{H} = (\mathcal{C}, f, \mathcal{D}, G)$. In hybrid system, a hybrid time point $(t, j) \in E$ is parameterized by both t , the amount of time passed since initiation, and j , the number of jumps that have occurred. A subset $E \subset \mathbb{R}_{\geq 0} \times \mathbb{Z}_{\geq 0}$ is a hybrid time domain if it is the union of a finite or infinite sequence of interval $[t_k, t_{k+1}] \times \{k\}$. A solution to \mathcal{H} is a function $\phi : E \rightarrow \mathbb{R}^n$ where ϕ satisfies the dynamics of \mathcal{H} , E is a hybrid time domain, and for each $j \in \mathbb{N}$, the function $t \mapsto \phi(t, j)$ is locally absolutely continuous on $I_j = \{t : (t, j) \in E\}$. $\phi(t, j)$ is called a hybrid arc. A hybrid arc ϕ is nontrivial if its domain contains at least two points, is maximal if it is not the truncation of another solution, and is complete if its domain is unbounded. Moreover, a hybrid arc ϕ is Zeno if it is complete and $\sup_t \text{dom } \phi < \infty$, is continuous if it is nontrivial and $\text{dom } \phi \subset \mathbb{R}_{\geq 0} \times \{0\}$, is eventually continuous if $J = \sup_j \text{dom } \phi < \infty$ and $\text{dom } \phi \cap (\mathbb{R}_{\geq 0} \times \{J\})$ contains at least two points, is discrete if it is nontrivial and $\text{dom } \phi \subset \{0\} \times \mathbb{Z}_{\geq 0}$, and is eventually discrete if $T = \sup_t \text{dom } \phi < \infty$ and $\text{dom } \phi \cap (\{T\} \times \mathbb{Z}_{\geq 0})$ contains at least two points. Given a set \mathcal{M} , we denote $\mathcal{S}_{\mathcal{H}}(\mathcal{M})$ the set of all maximal solutions ϕ to \mathcal{H} with $\phi(0, 0) \in \mathcal{M}$.

Some notions and results for the hybrid system \mathcal{H} from Goebel et al. (2012) which will be used in this paper are given as follows.

Definition 1. $\mathcal{H} = (\mathcal{C}, f, \mathcal{D}, G)$ satisfies the hybrid basic conditions if: (1) \mathcal{C} and \mathcal{D} are closed in \mathbb{R}^n ; (2) $f : \mathbb{R}^n \rightarrow \mathbb{R}^n$ is continuous and locally bounded on $\mathcal{C} \subset \text{dom } f$; and (3) $G : \mathbb{R}^n \rightrightarrows \mathbb{R}^n$ is outer-semicontinuous and locally bounded on $\mathcal{D} \subset \text{dom } G$.

Definition 2. A set $S \subset \mathbb{R}^n$ is said to be strongly forward invariant if for every $\phi \in \mathcal{S}_{\mathcal{H}}(S)$, $\text{rge } \phi \subset S$.

Definition 3. Given a set $S \subset \mathbb{R}^n$, a hybrid system \mathcal{H} on \mathbb{R}^n is pre-forward complete from S if every $\phi \in \mathcal{S}_{\mathcal{H}}(S)$ is either bounded or complete.

Definition 4. A compact set $\mathcal{A} \subset \mathbb{R}^n$ is said to be uniformly attractive from a set $S \subset \mathbb{R}^n$ if every $\phi \in \mathcal{S}_{\mathcal{H}}(S)$ is bounded and for every $\varepsilon > 0$ there exists $\tau > 0$ such that $|\phi(t, j)|_{\mathcal{A}} \leq \varepsilon$ for every $\phi \in \mathcal{S}_{\mathcal{H}}(S)$ and $(t, j) \in \text{dom } \phi$ with $t + j \geq \tau$.

Definition 5. A compact set $\mathcal{A} \subset \mathbb{R}^n$ is said to be

- stable for \mathcal{H} if for every $\varepsilon > 0$ there exists $\delta > 0$ such that every solution ϕ to \mathcal{H} with $|\phi(0, 0)|_{\mathcal{A}} \leq \delta$ satisfies $|\phi(t, j)|_{\mathcal{A}} \leq \varepsilon$ for all $(t, j) \in \text{dom } \phi$;

- locally attractive for \mathcal{H} if every maximal solution to \mathcal{H} is bounded and complete, and there exists $\mu > 0$ such that every solution ϕ to \mathcal{H} with $|\phi(0, 0)|_{\mathcal{A}} \leq \mu$ converges to \mathcal{A} , i.e., $\lim_{t+j \rightarrow \infty} |\phi(t, j)|_{\mathcal{A}} = 0$ holds;
- locally asymptotically stable for \mathcal{H} if it is both stable and locally attractive for \mathcal{H} .

Definition 6. Let $\mathcal{A} \subset \mathbb{R}^n$ be locally asymptotically stable for \mathcal{H} . Then the basin of attraction of \mathcal{A} , denoted by $\mathcal{B}_{\mathcal{A}}$, is the set of points such that every $\phi \in \mathcal{S}_{\mathcal{H}}(\mathcal{B}_{\mathcal{A}})$ is bounded, complete, and $\lim_{t+j \rightarrow \infty} |\phi(t, j)|_{\mathcal{A}} = 0$.

Definition 7. Given $\tau, \varepsilon > 0$, two hybrid arcs ϕ_1 and ϕ_2 are (τ, ε) -close if

- $\forall (t, j) \in \text{dom } \phi_1$ with $t + j \leq \tau$ there exists s such that $(s, j) \in \text{dom } \phi_2$, $|t - s| < \varepsilon$ and $|\phi_1(t, j) - \phi_2(s, j)| < \varepsilon$;
- $\forall (t, j) \in \text{dom } \phi_2$ with $t + j \leq \tau$ there exists s such that $(s, j) \in \text{dom } \phi_1$, $|t - s| < \varepsilon$ and $|\phi_2(t, j) - \phi_1(s, j)| < \varepsilon$.

Lemma 1 (Theorem 8.2 in Goebel et al. (2012)). Consider a continuous function $V : \mathbb{R}^n \rightarrow \mathbb{R}$, any functions $u_{\mathcal{C}}, u_{\mathcal{D}} : \mathbb{R}^n \rightarrow [-\infty, \infty]$, and a set $U \subset \mathbb{R}^n$ such that $u_{\mathcal{C}}(z) \leq 0$, $u_{\mathcal{D}}(z) \leq 0$ for every $z \in U$ and such that the growth of V along solutions to \mathcal{H} is bounded by $u_{\mathcal{C}}, u_{\mathcal{D}}$ on U . Let a precompact solution $\phi^* \in \mathcal{S}_{\mathcal{H}}$ be such that $\text{rge } \phi^* \subset U$. Then, for some $r \in V(U)$, ϕ^* approaches the nonempty set that is the largest weakly invariant subset of $V^{-1}(r) \cap U \cap [u_{\mathcal{C}}^{-1}(0) \cup (u_{\mathcal{D}}^{-1}(0) \cap G(u_{\mathcal{D}}^{-1}(0)))]$.

Lemma 2 (Proposition 7.5 in Goebel et al. (2012)). Let \mathcal{H} be nominally well-posed. Suppose that a compact set $\mathcal{A} \subset \mathbb{R}^n$ has the following properties: (1) it is strongly forward invariant, and (2) it is uniformly attractive from a neighborhood of itself, i.e., there exists $\mu > 0$ such that \mathcal{A} is uniformly attractive from $\mathcal{A} + \mu\mathbb{B}$. Then the compact set \mathcal{A} is locally asymptotically stable.

Lemma 3 (Proposition 6.34 in Goebel et al. (2012)). Let \mathcal{H} be well-posed. Suppose that \mathcal{H} is pre-forward complete from a compact set $K \subset \mathbb{R}^n$ and $\rho : \mathbb{R}^n \rightarrow \mathbb{R}_{\geq 0}$. Then for every $\varepsilon > 0$ and $\tau \geq 0$, there exists $\delta > 0$ with the following property: for every solution ϕ_{δ} to $\mathcal{H}_{\delta\rho}$ with $\phi_{\delta}(0, 0) \in K + \delta\mathbb{B}$, there exists a solution ϕ to \mathcal{H} with $\phi(0, 0) \in K$ such that ϕ_{δ} and ϕ are (τ, ε) -close.

2.3. Communication graph

We use a graph $\mathcal{G} = (\mathcal{V}, \mathcal{E}, \mathcal{W})$ to represent the interaction pattern of PCOs, where the node set $\mathcal{V} = \{1, 2, \dots, N\}$ denotes all oscillators. $\mathcal{E} \subset \mathcal{V} \times \mathcal{V}$ is the edge set, whose elements are such that $(i, j) \in \mathcal{E}$ holds if and only if node j can receive messages from node i . We assume that no self edge exists, i.e., $(i, i) \notin \mathcal{E}$. $\mathcal{W} = [w_{ij}] \in \mathbb{R}^{N \times N}$ is the weighted adjacency matrix of \mathcal{G} with $w_{ij} \geq 0$, where $w_{ij} > 0$ if and only if $(i, j) \in \mathcal{E}$ holds. The out-neighbor set of node i , which represents the set of nodes that can receive messages from node i , is denoted as $\mathcal{N}_i^{\text{out}} := \{j \in \mathcal{V} : (i, j) \in \mathcal{E}\}$.

We focus on chain graphs (both undirected and directed) and directed tree graphs which are defined as follows:

Definition 8. An undirected chain graph \mathcal{G} is a graph whose nodes can be indexed such that there exist two edges $(i, i + 1)$ and $(i + 1, i)$ between nodes i and $i + 1$ for $i = 1, 2, \dots, N - 1$.

Definition 9. A directed chain graph \mathcal{G} is a graph whose nodes can be indexed such that there is only one edge between nodes i and $i + 1$ for $i = 1, 2, \dots, N - 1$ and all edges are directed in the same direction. Without loss of generality, we suppose that the edge between nodes i and $i + 1$ is $(i, i + 1)$.

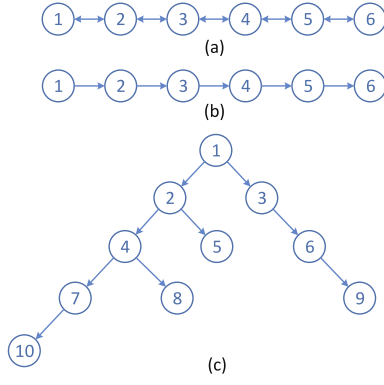


Fig. 1. Illustration of graphs: (a) undirected chain graph with six nodes; (b) directed chain graph with six nodes; (c) directed tree graph with ten nodes.

Definition 10. A directed tree graph \mathcal{G} is a cycle-free graph with a designated node as a root such that the root has exactly one directed chain to every other node.

Examples of undirected chain graph, directed chain graph, and directed tree graph are given in Fig. 1.

3. Problem statement

3.1. System description

We consider N PCOs interacting on a graph $\mathcal{G} = (\mathcal{V}, \mathcal{E}, \mathcal{W})$. Each oscillator is characterized by a phase variable $x_i \in [0, 2\pi]$ for each $i \in \mathcal{V}$. Each phase variable x_i evolves from 0 to 2π according to integrate-and-fire dynamics, i.e., $\dot{x}_i = \omega$, where $\omega \in \mathbb{R}_{>0}$ is the natural frequency of the oscillators. When x_i reaches 2π , oscillator i fires (emits a pulse) and resets x_i to 0, after which the cycle repeats. When a neighboring oscillator j receives the pulse from oscillator i , it shifts its phase according to its coupling strength $l_j \in (0, 1)$ (a scalar value) and its phase response function (PRF) F_j (Achuthan & Canavier, 2009; Canavier & Achuthan, 2010; Dror et al., 1999; Ermentrout, 1996; Hansel et al., 1995; Izhikevich, 2007), i.e., $x_j^+ = x_j + l_j F_j(x_j)$, where x_j^+ denotes the phase right after phase shift.

3.2. Hybrid model and dynamical properties

Due to the hybrid behavior of PCOs similar to Ferrante and Wang (2017) and Núñez et al. (2015a,b), we model them as a hybrid system \mathcal{H} with state $x = [x_1, \dots, x_N]^T$. To this end, we define the flow set \mathcal{C} and the flow map $f(x)$ as follows:

$$\mathcal{C} = [0, 2\pi]^N, \quad f(x) = \omega \mathbf{1}_N \quad \forall x \in \mathcal{C} \quad (2)$$

According to Núñez et al. (2015a,b), the jump set \mathcal{D} and the jump map $G(x)$ can be defined as the union of the individual jump sets \mathcal{D}_i and individual jump maps $G_i(x)$, respectively

$$\mathcal{D} := \bigcup_{i \in \mathcal{V}} \mathcal{D}_i, \quad G(x) := \bigcup_{i \in \mathcal{V}: x \in \mathcal{D}_i} G_i(x) \quad (3)$$

where \mathcal{D}_i is defined as $\mathcal{D}_i = \{x \in \mathcal{C} : x_i = 2\pi\}$ and $\forall x \in \mathcal{D}_i$, $G_i(x)$ is given by

$$G_i(x) = \{x^+ : x_i^+ = 0, x_j^+ \in x_j + w_{ij} F_j(x_j) \quad \forall j \neq i\} \quad (4)$$

Note $w_{ij} = l_j \in (0, 1)$ if $j \in \mathcal{N}_i^{\text{out}}$; otherwise, $w_{ij} = 0$.

To make \mathcal{H} an accurate description of PCOs, we make the following assumptions on the PRF F_j .

Assumption 1. The graph of F_j for $j \in \mathcal{V}$ is such that $\text{graph}(F_j) \subseteq \{(x_j, y_j) : x_j \in [0, 2\pi], -x_j \leq y_j \leq 2\pi - x_j\}$.

This assumption ensures that $G(\mathcal{D}) \subset \mathcal{C} \cup \mathcal{D} = \mathcal{C}$ since $l_j \in (0, 1)$ holds, which avoids the existence of solutions ending in finite time due to jumping outside \mathcal{C} .

Assumption 2. The PRF F_j for $j \in \mathcal{V}$ is an outer-semicontinuous set-valued map with $F_j(0) = F_j(2\pi) = 0$.

The constraint $F_j(0) = F_j(2\pi) = 0$ rules out discrete and eventually discrete solutions, meaning that PCOs will not fire continuously without rest (Núñez et al., 2015a, 2016). In fact, there are at most N consecutive jumps with no flow in between because an incoming pulse cannot trigger an oscillator who just fired to fire again under the constraint $F_j(0) = F_j(2\pi) = 0$.

The dynamical properties of \mathcal{H} are characterized as follows.

Proposition 1. Under Assumptions 1 and 2, we have

- (1) \mathcal{H} satisfies the hybrid basic conditions in Definition 1;
- (2) For every initial condition $\xi \in \mathcal{C} \cup \mathcal{D} = \mathcal{C}$, there exists at least one nontrivial solution to \mathcal{H} . In particular, every solution $\phi \in \mathcal{S}_{\mathcal{H}}(\mathcal{C})$ is maximal, complete, and non-Zeno;
- (3) For every solution $\phi \in \mathcal{S}_{\mathcal{H}}(\mathcal{C})$, $\sup_j \text{dom } \phi = \infty$ holds, which rules out the existence of continuous and eventually continuous solutions.

Proof. First we prove statement (1). According to the hybrid model in (2)–(4), \mathcal{C} and \mathcal{D} are closed, and f is continuous and locally bounded on \mathcal{C} . Also G is locally bounded since the PRF F_j satisfies Assumption 1. To prove G is outer-semicontinuous on \mathcal{D} , it suffices to show that $\text{graph}(G) = \bigcup_{i \in \mathcal{V}} \{(x, x^+) : x \in \mathcal{D}_i, x^+ \in G_i(x)\}$ is closed. According to Núñez et al. (2015a,b, 2016), the outer-semicontinuity of F_j in Assumption 2 ensures that $\{(x, x^+) : x \in \mathcal{D}_i, x^+ \in G_i(x)\}$ is closed for $i \in \mathcal{V}$, and hence G is outer-semicontinuous on \mathcal{D} . Therefore, \mathcal{H} satisfies the hybrid basic conditions in Definition 1.

Next we prove statement (2). Since \mathcal{H} satisfies the hybrid basic conditions, according to Proposition 6.10 in Goebel et al. (2012), there exists at least one nontrivial solution to \mathcal{H} for every initial condition $\xi \in \mathcal{C} \cup \mathcal{D} = \mathcal{C}$, and every solution $\phi \in \mathcal{S}_{\mathcal{H}}(\mathcal{C})$ is complete due to the facts that $G(\mathcal{D}) \subset \mathcal{C} \cup \mathcal{D} = \mathcal{C}$ holds and \mathcal{C} is compact, which also implies that ϕ is maximal. Since $G(\mathcal{D}) \subset \mathcal{C}$ holds, we have $\text{rge } \phi \subset \mathcal{C}$ for every $\phi \in \mathcal{S}_{\mathcal{H}}(\mathcal{C})$. So, according to Definition 2, \mathcal{C} is strongly forward invariant. Since the constraint $F_j(0) = F_j(2\pi) = 0$ in Assumption 2 rules out complete discrete solutions, from Proposition 6.35 in Goebel et al. (2012) we have that $\mathcal{S}_{\mathcal{H}}(\mathcal{C})$ is uniformly non-Zeno, which means that every $\phi \in \mathcal{S}_{\mathcal{H}}(\mathcal{C})$ is non-Zeno.

Finally we prove statement (3). Since every $\phi \in \mathcal{S}_{\mathcal{H}}(\mathcal{C})$ is complete and the length of each flow interval is at most $\frac{2\pi}{\omega}$, we have $\sup_j \text{dom } \phi = \infty$. So the existence of continuous and eventually continuous solutions is ruled out. ■

Remark 1. As indicated in Núñez et al. (2015b), such hybrid model \mathcal{H} is able to handle multiple simultaneous pulses, i.e., if an oscillator receives multiple pulses simultaneously, it will respond to these pulses sequentially (in whatever order), but the oscillation behavior is the same as if the components of x jumped simultaneously.

3.3. General delay-advance PRF

In this paper, we consider general delay-advance PRFs.

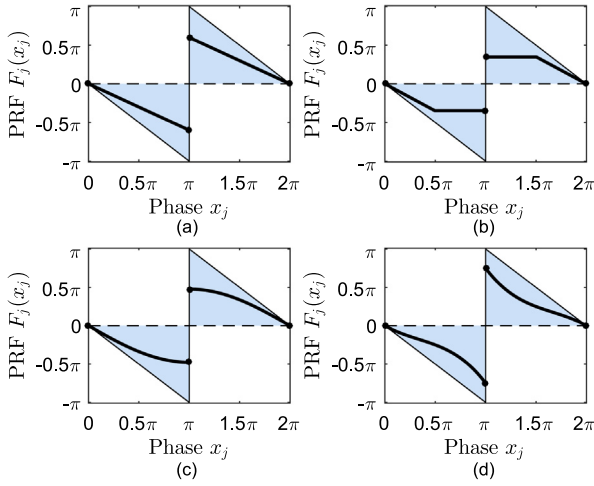


Fig. 2. Examples of the general delay-advance PRF $F_j(x_j)$.

Assumption 3. A delay-advance PRF F_j is such that

$$F_j(x_j) = \begin{cases} F_j^{(1)}(x_j), & \text{if } x_j \in [0, \pi) \\ \{F_j^{(1)}(\pi), F_j^{(2)}(\pi)\}, & \text{if } x_j = \pi \\ F_j^{(2)}(x_j), & \text{if } x_j \in (\pi, 2\pi] \end{cases} \quad (5)$$

where $F_j^{(1)}(x_j)$ and $F_j^{(2)}(x_j)$ are continuous functions on $[0, \pi]$ and $[\pi, 2\pi]$, respectively, and satisfy

$$\begin{cases} F_j^{(1)}(0) = 0, & F_j^{(1)}(x_j) \in [-x_j, 0) \text{ if } x_j \in (0, \pi) \\ F_j^{(2)}(2\pi) = 0, & F_j^{(2)}(x_j) \in (0, 2\pi - x_j] \text{ if } x_j \in [\pi, 2\pi) \end{cases} \quad (6)$$

Similar to Núñez et al. (2015a,b, 2016), F_j is an outer-semicontinuous set-valued map. Note that oscillators with phases in $(0, \pi)$ will be delayed after receiving a pulse, meaning that their phases will be pushed closer to zero by each pulse received, whereas oscillators with phases in $(\pi, 2\pi)$ will be advanced, meaning that their phases will be pushed toward 2π by each pulse. If an oscillator has phase 0 (or 2π) upon receiving a pulse, its phase is unchanged by the pulse.

Since Assumption 3 implies Assumptions 1 and 2, the properties of \mathcal{H} in Proposition 1 still hold. Several examples of delay-advance PRF are illustrated in Fig. 2.

Remark 2. It is worth noting that our PRF can be heterogeneous and is also very general. In fact, it includes the PRFs used in Kannapan and Bullo (2016), Núñez et al. (2015a,b), Wang and Doyle III (2012), Wang et al. (2012, 2013a) and Yun, Ha, and Kwak (2015) as special cases. Therefore, our work has broad potential applications in engineered systems (Wang, Núñez, & Doyle III, 2013b) as well as biological systems (Izhikevich, 2007).

4. Global synchronization of PCOs

In this section, we analyze global PCO synchronization on both chain and directed tree graphs, and provide robustness analysis in the presence of frequency perturbations.

To this end, we first define the synchronization set \mathcal{A} :

$$\mathcal{A} = \{x \in \mathcal{C} : |x_i - x_j| = 0 \text{ or } |x_i - x_j| = 2\pi, \forall i, j \in \mathcal{V}\} \quad (7)$$

The PCO network synchronizes if the state x converges to the synchronization set \mathcal{A} . Note that \mathcal{A} is compact since it is closed and bounded (included in \mathcal{C} that is bounded).

In the following, we refer to an arc as a connected subset of $[0, 2\pi]$ where 0 and 2π are associated with each other. So phase

difference Δ_i that measures the length of the shorter arc between x_i and x_{i+1} on the unit cycle is given by

$$\Delta_i = \min\{|x_i - x_{i+1}|, 2\pi - |x_i - x_{i+1}|\} \quad (8)$$

where x_{N+1} is mapped to x_1 in Δ_N . It is straightforward to show that Δ_i satisfies $0 \leq \Delta_i \leq \pi$.

To measure the degree of synchronization, we define L as

$$L = \sum_{i=1}^N \Delta_i \quad (9)$$

Since $0 \leq \Delta_i \leq \pi$ holds, we have $0 \leq L \leq N\pi$. Note that both Δ_i for $i \in \mathcal{V}$ and L are dependent on x , and L is positive definite with respect to \mathcal{A} on $\mathcal{C} \cup \mathcal{D} = \mathcal{C}$ because $L = 0$ holds if and only if $\Delta_1 = \Delta_2 = \dots = \Delta_N = 0$ holds. Therefore, in order to prove synchronization, we only need to show that L will converge to 0. It is worth noting that L is continuous in $x \in \mathcal{C}$ but not differentiable with respect to it.

4.1. Global synchronization on undirected chain graphs

Lemma 4. For N PCOs interacting on an undirected chain, if the PRF $F_j(x_j)$ satisfies Assumption 3 and $l_j \in (0, 1)$ holds for all $j \in \mathcal{V}$, then L in (9) is nonincreasing along any solution $\phi \in \mathcal{S}_{\mathcal{H}}(\mathcal{C})$.

Proof. Since there is no interaction among oscillators during flows and all oscillators have the same natural frequency, we have that L is constant during flows and its dynamics only depends on jumps. Without loss of generality, we assume that at time (t_i^*, k_i^*) , we have $x(t_i^*, k_i^*) \in \mathcal{D}_i$, i.e., $x_i(t_i^*, k_i^*) = 2\pi$. (In the following, we omit time index (t_i^*, k_i^*) to simplify the notation.) When oscillator i fires and resets its phase to $x_i^+ = 0$, an oscillator $j \in \mathcal{N}_i^{\text{out}}$ has $x_j^+ \in x_j + l_j F_j(x_j)$ but an oscillator $j \notin \mathcal{N}_i^{\text{out}}$ still has $x_j^+ = x_j$.

For the undirected chain graph, we call oscillator $i - 1$ as the left-neighbor of oscillator i for $i = 2, 3, \dots, N$, and call oscillator $i + 1$ as the right-neighbor of oscillator i for $i = 1, 2, \dots, N - 1$. Upon the firing of oscillator i , if the left-neighbor oscillator $i - 1$ exists, it will update its phase and affect Δ_{i-2} and Δ_{i-1} . Note that for $i = 2$, Δ_{i-2} is mapped to Δ_N . Similarly, if the right-neighbor oscillator $i + 1$ exists, Δ_i and Δ_{i+1} will be affected. No other Δ_k s will be affected by this pulse, i.e., $\Delta_k^+ = \Delta_k$ holds for $k \notin \{i - 2, i - 1, i, i + 1\}$ where Δ_k^+ denotes the phase difference between oscillators k and $k + 1$ after the jump. Therefore, we only need to consider two situations when oscillator i fires, i.e., how Δ_{i-2} and Δ_{i-1} change if the left-neighbor oscillator $i - 1$ exists and how Δ_i and Δ_{i+1} change if the right-neighbor oscillator $i + 1$ exists.

Situation I: If the left-neighbor oscillator $i - 1$ exists, from (4) and (5) we have

$$x_{i-1}^+ = \begin{cases} x_{i-1} + l_{i-1} F_{i-1}^{(1)}(x_{i-1}), & \text{if } x_{i-1} \in [0, \pi) \\ x_{i-1} + l_{i-1} F_{i-1}^{(2)}(x_{i-1}), & \text{if } x_{i-1} \in [\pi, 2\pi] \end{cases} \quad (10)$$

To facilitate the proof, we use a nonnegative variable δ_{i-1} to denote the jump magnitude of oscillator $i - 1$. According to (6) and $l_{i-1} \in (0, 1)$, δ_{i-1} is determined by

$$\delta_{i-1} = \begin{cases} -l_{i-1} F_{i-1}^{(1)}(x_{i-1}), & \text{if } x_{i-1} \in [0, \pi) \\ l_{i-1} F_{i-1}^{(2)}(x_{i-1}), & \text{if } x_{i-1} \in [\pi, 2\pi] \end{cases} \quad (11)$$

Since $x_i = 2\pi$ and $x_i^+ = 0$ hold, from (10) and (11) we know that oscillator $i - 1$ jumps δ_{i-1} towards oscillator i , as illustrated in Fig. 3. So we have $\Delta_{i-1}^+ = \Delta_{i-1} - \delta_{i-1}$.

Now we analyze how Δ_{i-2} changes upon oscillator i 's firing. Note that $x_{i-2}^+ = x_{i-2}$ holds as $i - 2 \notin \mathcal{N}_i^{\text{out}}$. According to the

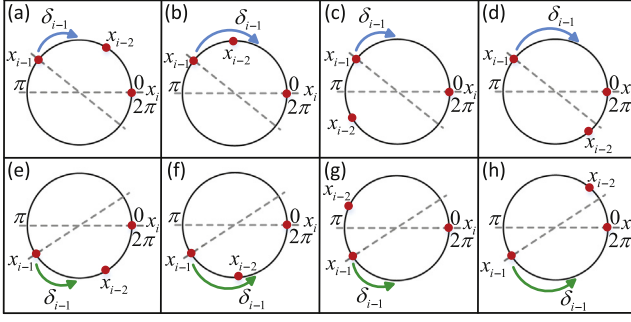


Fig. 3. Illustration of Situation I.

direction of oscillator $i - 1$'s jump and the relationship between δ_{i-1} and Δ_{i-2} , we have the four following cases:

Case 1: If oscillator $i - 1$ jumps δ_{i-1} towards oscillator $i - 2$ and $\delta_{i-1} \leq \Delta_{i-2}$ holds (cf. Fig. 3(a) and (e)), we have $\Delta_{i-2}^+ = \Delta_{i-2} - \delta_{i-1}$, which leads to

$$\Delta_{i-1}^+ + \Delta_{i-2}^+ = \Delta_{i-1} + \Delta_{i-2} - 2\delta_{i-1} \leq \Delta_{i-1} + \Delta_{i-2} \quad (12)$$

Note that the equality holds if and only if $\delta_{i-1} = 0$ exists, i.e., $\Delta_{i-1}^+ + \Delta_{i-2}^+ = \Delta_{i-1} + \Delta_{i-2}$ holds if and only if $\Delta_{i-2}^+ = \Delta_{i-2} - \delta_{i-1} = \Delta_{i-2} + \delta_{i-1}$ holds.

Case 2: If oscillator $i - 1$ jumps δ_{i-1} towards oscillator $i - 2$ and $\delta_{i-1} > \Delta_{i-2}$ holds (cf. Fig. 3(b) and (f)), we have $\Delta_{i-2}^+ = \delta_{i-1} - \Delta_{i-2}$. So it follows

$$\Delta_{i-1}^+ + \Delta_{i-2}^+ = \Delta_{i-1} - \Delta_{i-2} \leq \Delta_{i-1} + \Delta_{i-2} \quad (13)$$

where the equality occurs when $\Delta_{i-2} = 0$, i.e., $\Delta_{i-1}^+ + \Delta_{i-2}^+ = \Delta_{i-1} + \Delta_{i-2}$ holds if and only if $\Delta_{i-2}^+ = \delta_{i-1} - \Delta_{i-2} = \Delta_{i-2} + \delta_{i-1}$ holds.

Case 3: If oscillator $i - 1$ jumps δ_{i-1} away from oscillator $i - 2$ and $\Delta_{i-2} + \delta_{i-1} \leq \pi$ holds (cf. Fig. 3(c) and (g)), we have $\Delta_{i-2}^+ = \Delta_{i-2} + \delta_{i-1}$, which leads to

$$\Delta_{i-1}^+ + \Delta_{i-2}^+ = \Delta_{i-1} + \Delta_{i-2} \quad (14)$$

Case 4: If oscillator $i - 1$ jumps δ_{i-1} away from oscillator $i - 2$ and $\Delta_{i-2} + \delta_{i-1} > \pi$ holds (cf. Fig. 3(d) and (h)), we have $\Delta_{i-2}^+ = 2\pi - \Delta_{i-2} - \delta_{i-1} < \pi < \Delta_{i-2} + \delta_{i-1}$ and

$$\begin{aligned} \Delta_{i-1}^+ + \Delta_{i-2}^+ &< (\Delta_{i-1} - \delta_{i-1}) + (\Delta_{i-2} + \delta_{i-1}) \\ &= \Delta_{i-1} + \Delta_{i-2} \end{aligned} \quad (15)$$

Summarizing the above four cases, we have

$$\Delta_{i-1}^+ + \Delta_{i-2}^+ \leq \Delta_{i-1} + \Delta_{i-2} \quad (16)$$

where the equality occurs when $\Delta_{i-2}^+ = \Delta_{i-2} + \delta_{i-1}$.

Situation II: If the right-neighbor oscillator $i + 1$ exists, it will update its phase according to (4) and (5) as follows

$$x_{i+1}^+ = \begin{cases} x_{i+1} + l_{i+1}F_{i+1}^{(1)}(x_{i+1}), & \text{if } x_{i+1} \in [0, \pi] \\ x_{i+1} + l_{i+1}F_{i+1}^{(2)}(x_{i+1}), & \text{if } x_{i+1} \in [\pi, 2\pi] \end{cases} \quad (17)$$

Also the nonnegative magnitude of oscillator $i + 1$'s phase jump (denoted by δ_{i+1}) is given as

$$\delta_{i+1} = \begin{cases} -l_{i+1}F_{i+1}^{(1)}(x_{i+1}), & \text{if } x_{i+1} \in [0, \pi] \\ l_{i+1}F_{i+1}^{(2)}(x_{i+1}), & \text{if } x_{i+1} \in [\pi, 2\pi] \end{cases} \quad (18)$$

Since $x_i = 2\pi$ and $x_i^+ = 0$ hold, and oscillator $i + 1$ jumps δ_{i+1} towards oscillator i , we have $\Delta_i^+ = \Delta_i - \delta_{i+1}$.

According to the relationship between δ_{i+1} and Δ_{i+1} , there are also four cases on the change of Δ_{i+1} . Similar to Situation I, we can obtain the following result:

$$\Delta_i^+ + \Delta_{i+1}^+ \leq \Delta_i + \Delta_{i+1} \quad (19)$$

where the equality occurs when $\Delta_{i+1}^+ = \Delta_{i+1} + \delta_{i+1}$.

Summarizing Situation I and Situation II, we can see that L will not increase during jumps. Therefore, L is nonincreasing along any solution $\phi \in S_{\mathcal{H}}(C)$. ■

Now we are in position to introduce our results for global synchronization on undirected chain graphs.

Theorem 1. For N PCOs interacting on an undirected chain, if the PRF $F_j(x_j)$ satisfies Assumption 3 and $l_j \in (0, 1)$ holds for all $j \in \mathcal{V}$, then the synchronization set \mathcal{A} in (7) is globally asymptotically stable, i.e., global synchronization can be achieved from an arbitrary initial condition.

Proof. According to the derivation in Lemma 4, the continuous function L in (9) is constant during flows and will not increase during jumps, which implies that $L(g) - L(x) \leq 0$ holds for all $x \in \mathcal{D}$ and $g \in G(x)$. Defining $u_c(x) = 0$ for each $x \in \mathcal{C}$ and $u_c(x) = -\infty$ otherwise; $u_D(x) = \max_{g \in G(x)} \{L(g) - L(x)\} \leq 0$ for each $x \in \mathcal{D}$ and $u_D(x) = -\infty$ otherwise, we can bound the growth of L along solutions by u_c and u_D on \mathcal{C} (Goebel et al., 2012). According to Proposition 1, every solution $\phi \in S_{\mathcal{H}}(C)$ is precompact, i.e., complete and bounded, and satisfies $\text{rge } \phi \subset \mathcal{C} \cup \mathcal{D} = \mathcal{C}$. From Lemma 1, for some $r \in L(\mathcal{C}) = [0, N\pi]$, ϕ approaches the nonempty set that is the largest weakly invariant subset of $L^{-1}(r) \cap \mathcal{C} \cap [u_c^{-1}(0) \cup (u_D^{-1}(0) \cap G(u_D^{-1}(0)))]$ where $L^{-1}(r)$ denotes the r -level set of L defined in Section 2.1 (note that Lemma 1 does not need L to be continuously differentiable in $x \in \mathcal{C}$ (Goebel et al., 2012)). Since $u_c^{-1}(0) = \mathcal{C}$ and $u_D^{-1}(0) \cap G(u_D^{-1}(0)) \subset \mathcal{D}$ hold, we have $L^{-1}(r) \cap \mathcal{C} \cap [u_c^{-1}(0) \cup (u_D^{-1}(0) \cap G(u_D^{-1}(0)))] = L^{-1}(r) \cap \mathcal{C}$.

According to Lemma 5 in Appendix A, L cannot be retained at any nonzero value along a complete solution ϕ . So the largest weakly invariant subset of $L^{-1}(r) \cap \mathcal{C}$ is empty for every $r \in (0, N\pi]$, which implies that every solution $\phi \in S_{\mathcal{H}}(C)$ approaches $L^{-1}(0) \cap \mathcal{C} = \mathcal{A}$.

Next we show that \mathcal{A} is locally asymptotically stable. Since every solution $\phi \in S_{\mathcal{H}}(C)$ approaches \mathcal{A} , from Definition 4, \mathcal{A} is uniformly attractive from \mathcal{C} . As Assumption 2 guarantees that $\text{rge } \phi \subset \mathcal{A}$ for every $\phi \in S_{\mathcal{H}}(\mathcal{A})$, \mathcal{A} is strongly forward invariant according to Definition 2. Therefore, from Lemma 2, \mathcal{A} is locally asymptotically stable.

To show \mathcal{A} is globally asymptotically stable, it suffices to show that \mathcal{A} 's basin of attraction $\mathcal{B}_{\mathcal{A}}$ contains $\mathcal{C} \cup \mathcal{D} = \mathcal{C}$. Since we have shown that the largest weakly invariant subset of $L^{-1}(r) \cap \mathcal{C}$ is empty for every $r \in (0, N\pi]$ and every solution $\phi \in S_{\mathcal{H}}(C)$ approaches \mathcal{A} , according to Definition 6, \mathcal{A} 's basin of attraction $\mathcal{B}_{\mathcal{A}}$ contains \mathcal{C} . Therefore, \mathcal{A} is globally asymptotically stable.

In summary, \mathcal{A} is globally asymptotically stable, meaning that global synchronization can be achieved from an arbitrary initial condition. ■

Remark 3. Because using four phase differences (Δ_{i-2} , Δ_{i-1} , Δ_i , and Δ_{i+1} , which requires $N \geq 4$) is essential to describe and characterize the dynamics of a general number of N oscillators in a uniform manner, we assumed $N \geq 4$ in the proof. However, the results are also applicable to $N = 2$ and $N = 3$. In fact, following the analysis in Lemma 4, we can obtain that L is non-increasing when $N = 2$ or 3 . Then using the Invariance Principle based derivation in Theorem 1 gives the convergence of L to 0 and thus the achievement of global synchronization for $N = 2$ and 3 .

Remark 4. Compared with existing results in [Goel and Ermentrout \(2002\)](#) which show that local synchronization on chain graphs can be obtained as long as the coupling is not too strong, our results can guarantee global synchronization under any coupling strength between zero and one.

Remark 5. It is worth noting that different from local PCO synchronization analysis ([Goel & Ermentrout, 2002](#); [Hong & Scaglione, 2005](#)) and global PCO synchronization analysis under all-to-all topology ([Canavier & Tikidji-Hamburyan, 2017](#); [Núñez et al., 2015a](#)) where the firing order is time-invariant, the coupling strength $l \in (0, 1)$ cannot guarantee invariant firing order in our considered scenarios, as confirmed by numerical simulations in [Fig. 5](#).

4.2. Global synchronization on directed chain and tree graphs

In this subsection, we extend the global synchronization results to directed chain and tree graphs.

Corollary 1. For N PCOs interacting on a directed chain, if the PRF $F_j(x_j)$ satisfies [Assumption 3](#) and $l_j \in (0, 1)$ holds for all $j \in \mathcal{V}$, then the synchronization set \mathcal{A} in (7) is globally asymptotically stable, i.e., global synchronization can be achieved from an arbitrary initial condition.

Proof. The proof is similar to [Theorem 1](#) and omitted. ■

Remark 6. Different from the cycle graph in [Núñez et al. \(2015b\)](#) where a strong enough coupling strength is required, global synchronization can be achieved here under any coupling strength between zero and one. This is because in the chain case, the absence of interaction between oscillators 1 and N allows Δ_N to increase freely until it triggers L to decrease; in other words, the absence of interaction between oscillators 1 and N breaks the symmetry of the chain graph ([Golubitsky & Stewart, 2003](#)), which is key to remove undesired equilibria where L keeps unchanged. In comparison, the symmetry of the cycle graph can make L stay at some undesired equilibria under a weak coupling strength. So a strong enough coupling strength is required in the cycle graph case to achieve global synchronization.

Corollary 2. For N PCOs interacting on a directed tree, if the PRF $F_j(x_j)$ satisfies [Assumption 3](#) and $l_j \in (0, 1)$ holds for all $j \in \mathcal{V}$, then global synchronization can be achieved from an arbitrary initial condition.

Proof. Suppose in a directed tree graph there are m nodes without any out-neighbors which are represented as v_1, v_2, \dots, v_m . Take the graph in [Fig. 1\(c\)](#) as an example, nodes 5, 8, 9, and 10 do not have any out-neighbors. According to [Definition 10](#), for every node v_i ($i = 1, 2, \dots, m$) there is a unique directed chain from the root v_r to node v_i . So the directed tree graph is composed of m directed chains. Note that for every directed chain from the root v_r to node v_i , it is not affected by oscillators outside the chain. So the m directed chains are decoupled from each other. According to [Corollary 1](#), global synchronization can be achieved on the directed chain from an arbitrary initial condition if $F_j(x_j)$ satisfies [Assumption 3](#) and if $l_j \in (0, 1)$ holds. Adding the fact that the root oscillator v_r belongs to all m directed chains implies synchronization of all PCOs. ■

Remark 7. Different from the arguments in the proofs of [Corollaries 1](#) and [2](#), an alternative approach to proving global synchronization on direct chain (and tree) graphs is using inductive reasoning based on the following two facts: first, a parent node

can affect its child node but a child node never affects its parent node; secondly, under the given piecewise continuous delay-advance PRF (with values being nonzero in $(0, 2\pi)$), the phases of all oscillators on a directed chain will be reduced to within a half cycle, which always leads to synchronization (cf. [Theorem 2](#) in [Proskurnikov and Cao \(2017\)](#)).

Remark 8. Different from the “probability-one synchronization” in [Klinglmayr et al. \(2017, 2012\)](#) and [Lyu \(2015\)](#) where oscillators synchronize with probability one under a stochastic phase-responding mechanism and the “almost global synchronization” in [Chen \(1994\)](#), [Mathar and Matfeldt \(1996\)](#) and [Mirollo and Strogatz \(1990\)](#) where synchronization is guaranteed for all initial conditions except a set of Lebesgue-measure zero, our studied global synchronization is achieved in a deterministic manner from any initial condition, which is not only important theoretically but also mandatory in many safety-critical applications. A typical application justifying the necessity of deterministic global synchronization is synchronization based motion coordination of AUV (autonomous underwater vehicles) ([Paley, Leonard, Sepulchre, Grunbaum, & Parrish, 2007](#)) and UAV (unmanned aerial vehicles) ([Valbuena, Cruz, Figueroa, Sorrentino, & Fierro, 2014](#)). In such an application, even one single failure in synchronization might be too costly in money, time, energy, or even lives (cf. the multi-UAV based target engagement problem in [Furukawa, Durrant-Whyte, Dissanayake, and Sukkarieh \(2003\)](#)).

4.3. Robustness analysis for frequency perturbations

In this subsection, we analyze the robustness property of PCOs under small frequency perturbations on the natural frequency ω . It is worth noting that robustness is important since frequency perturbations are unavoidable and under an inappropriate synchronization mechanism, even a small difference in natural frequency may accumulate and lead to large phase differences. The hybrid systems model with frequency perturbations is given as follows:

$$\mathcal{H}_p : \begin{cases} \dot{x} = \omega \mathbf{1}_N + p, & x \in \mathcal{C} \\ x^+ \in G(x), & x \in \mathcal{D} \end{cases} \quad (20)$$

where $p = [p_1, \dots, p_N]^T$ represents the frequency perturbations. Using the notion of (τ, ε) -closeness given in [Definition 7](#) in [Section 2.2](#), we have the following result:

Theorem 2. Consider N PCOs with frequency perturbations as described by \mathcal{H}_p in (20). For every $\varepsilon > 0$, $\tau \geq 0$, and $\rho : \mathbb{R}^N \rightarrow \mathbb{R}_{\geq 0}$, there exists a scalar $\sigma > 0$ such that under any $p \in \sigma\rho(x)\mathbb{B}$ every solution ϕ_p to \mathcal{H}_p from \mathcal{C} is (τ, ε) -close to a solution ϕ to the perturbation-free dynamics \mathcal{H} .

Proof. According to [Proposition 1](#) in [Section 3.2](#), \mathcal{H} satisfies the hybrid basic conditions, and is pre-forward complete from the compact set \mathcal{C} since every $\phi \in \mathcal{S}_{\mathcal{H}}(\mathcal{C})$ is complete (see [Definition 3](#)). So from [Lemma 3](#), for every $\varepsilon > 0$, $\tau \geq 0$, and $\rho : \mathbb{R}^N \rightarrow \mathbb{R}_{\geq 0}$, there exists a scalar $\sigma > 0$ with the following property: for every solution ϕ_σ to $\mathcal{H}_{\sigma\rho}$ from \mathcal{C} , there exists a solution ϕ to \mathcal{H} from \mathcal{C} such that ϕ_σ and ϕ are (τ, ε) -close, where $\mathcal{H}_{\sigma\rho} = (\mathcal{C}, f_{\sigma\rho}, \mathcal{D}, G)$ is the $\sigma\rho$ -perturbation of \mathcal{H} and $f_{\sigma\rho}(x) = f(x) + \sigma\rho(x)\mathbb{B} = \omega\mathbf{1}_N + \sigma\rho(x)\mathbb{B}$ for every $x \in \mathcal{C}$. Note that if $p \in \sigma\rho(x)\mathbb{B}$, every solution ϕ_p to \mathcal{H}_p from \mathcal{C} is in fact the solution to $\mathcal{H}_{\sigma\rho}$, which implies that ϕ_p and ϕ are (τ, ε) -close. ■

According to [Theorem 2](#), the behavior of perturbed PCOs is close to the perturbation-free case, i.e., the solutions to the perturbed PCOs converge to the neighborhood of the synchronization set \mathcal{A} . Therefore, the phases of oscillators will remain close to each other under small frequency perturbations.

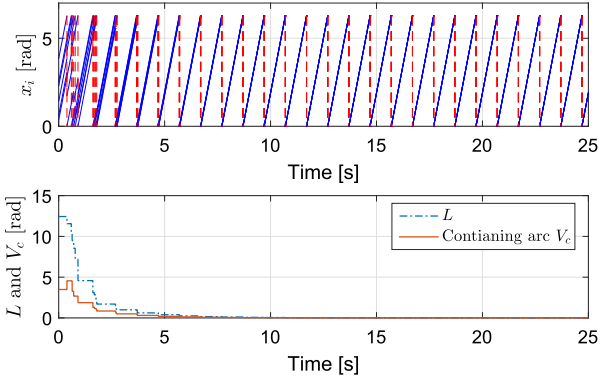


Fig. 4. Evolutions of phases and L for PCOs on an undirected chain graph.

5. Numerical experiments

5.1. Unperturbed case

We first considered the unperturbed case, i.e., all oscillators had an identical frequency $\omega = 2\pi$.

First we considered $N = 6$ PCOs on an undirected chain graph. Oscillators 1, ..., 6 adopted the PRFs (a), (b), (c), (d), (a), and (b) in Fig. 2, respectively. The respective analytical expressions of these PRFs are given below.

$$(a) : F_j(x_j) = \begin{cases} -0.6x_j, & \text{if } x_j \in [0, \pi) \\ \{-0.6\pi, 0.6\pi\}, & \text{if } x_j = \pi \\ 0.6(2\pi - x_j), & \text{if } x_j \in (\pi, 2\pi] \end{cases} \quad (21)$$

$$(b) : F_j(x_j) = \begin{cases} -0.7x_j, & \text{if } x_j \in [0, \frac{\pi}{2}) \\ -0.35\pi, & \text{if } x_j \in [\frac{\pi}{2}, \pi) \\ \{-0.35\pi, 0.35\pi\}, & \text{if } x_j = \pi \\ 0.35\pi, & \text{if } x_j \in (\pi, \frac{3\pi}{2}) \\ 0.7(2\pi - x_j), & \text{if } x_j \in (\frac{3\pi}{2}, 2\pi] \end{cases} \quad (22)$$

$$(c) : F_j(x_j) = \begin{cases} -1.5 \sin(0.5x_j), & \text{if } x_j \in [0, \pi) \\ \{-1.5, 1.5\}, & \text{if } x_j = \pi \\ 1.5 \sin(0.5x_j), & \text{if } x_j \in (\pi, 2\pi] \end{cases} \quad (23)$$

$$(d) : F_j(x_j) = \begin{cases} -x_j^3/\pi^2 + x_j^2/\pi - 0.75x_j, & \text{if } x_j \in [0, \pi) \\ \{-0.75\pi, 0.75\pi\}, & \text{if } x_j = \pi \\ -x_j^3/\pi^2 + 5x_j^2/\pi - 8.75x_j + 5.5\pi, & \text{if } x_j \in (\pi, 2\pi] \end{cases} \quad (24)$$

The coupling strength l_1, \dots, l_6 were set to 0.4, 0.5, 0.6, 0.6, 0.5, and 0.4, respectively. The initial phase $x(0, 0)$ was randomly chosen from $\mathcal{C} \cup \mathcal{D}$. Fig. 4 shows the evolutions of phases and L . It can be seen that L converged to 0, which confirmed Theorem 1.

From the lower plot of Fig. 4, we can also see that the length of the shortest containing arc V_c , which is widely used as a Lyapunov function in local synchronization analysis (Kannapan & Bullo, 2016; Núñez et al., 2015a, 2016; Proskurnikov & Cao, 2017), is not appropriate for global PCO synchronization as it may not decrease

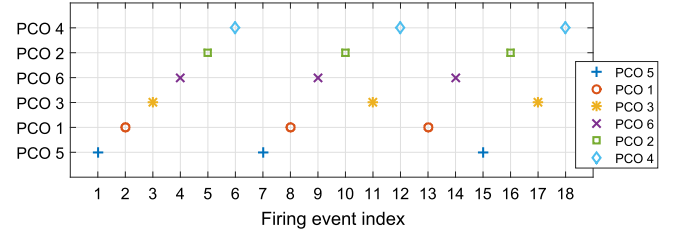


Fig. 5. Firing order of PCOs on the undirected chain graph.

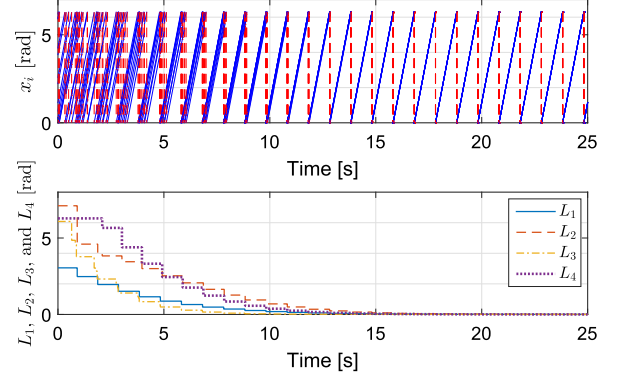


Fig. 6. Evolutions of phases, L_1 , L_2 , L_3 , and L_4 for PCOs on a directed tree graph. PCOs synchronized as L_1 , L_2 , L_3 , and L_4 converged to 0.

monotonically. Along the same line, the firing order which is invariant in Canavier and Tikidji-Hamburyan (2017), Goel and Ermentrout (2002), Hong and Scaglione (2005), and Núñez et al. (2015a), is not constant in the considered dynamics as exemplified in Fig. 5. These unique properties of chain and directed tree PCOs corroborate the novelty and importance of our results.

Then we considered $N = 10$ PCOs on a directed tree graph, as illustrated in Fig. 1(c). There are 4 directed chains in this graph, namely, oscillators $1 \rightarrow 2 \rightarrow 5$, oscillators $1 \rightarrow 2 \rightarrow 4 \rightarrow 8$, oscillators $1 \rightarrow 3 \rightarrow 6 \rightarrow 9$, and oscillators $1 \rightarrow 2 \rightarrow 4 \rightarrow 7 \rightarrow 10$. The same as (9), L_1, L_2, L_3 , and L_4 were defined to measure the degree of synchronization corresponding to the 4 directed chains, respectively. Oscillators 1, ..., 10 adopted the PRFs (a), (b), (c), (d), (a), (b), (c), (d), (a), and (b) in Fig. 2, respectively. The coupling strength l_1, \dots, l_{10} were set to 0.6, 0.5, 0.4, 0.6, 0.5, 0.4, 0.6, 0.5, 0.4, and 0.6, respectively. The initial phase $x(0, 0)$ was randomly chosen from $\mathcal{C} \cup \mathcal{D}$. The convergence of L_i ($i = 1, \dots, 4$) to zero in Fig. 6 implies the synchronization of the i th directed chain, which confirmed Corollary 1. The simultaneous synchronization of all four directed chains also means synchronization of the entire directed tree graph, which confirmed Corollary 2.

5.2. Perturbed case

We considered $N = 6$ PCOs on an undirected chain graph with frequency perturbations on oscillator k set to $p_k = 0.5 \sin(2\pi t + 2\pi k/N)$. The other settings were the same as the undirected chain case. The evolutions of phases and L are shown in Fig. 7. It can be seen that the perturbed behaviors did not differ too much from the unperturbed case in Fig. 4, and the solution converged to a neighborhood of the synchronization set \mathcal{A} as L approached a ball containing zero, which confirmed Theorem 2.

6. Conclusions

The global synchronization of PCOs interacting on chain and directed tree graphs was addressed. It was proven that PCOs can

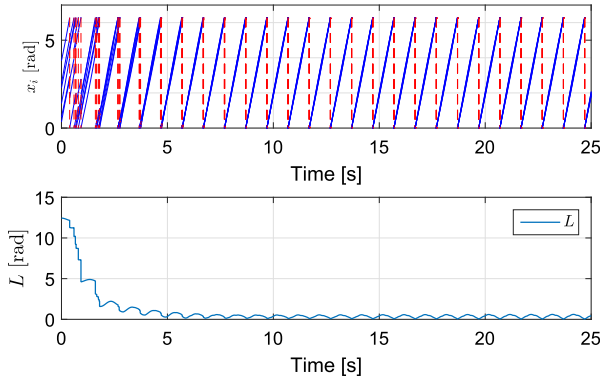


Fig. 7. Evolutions of phases and L for PCOs on an undirected chain graph under frequency perturbations.

be synchronized from an arbitrary initial phase distribution under heterogeneous phase response functions and coupling strengths. The results are also applicable when oscillators are heterogeneous and subject to time-varying perturbations on their natural frequencies. Note that different from existing global synchronization results, the coupling strengths in our results can be freely chosen between zero and one, which is desirable since a very strong coupling strength, although can bring fast convergence, has been shown to be detrimental to the robustness of synchronization to disturbances. Given that a very weak coupling may not be desirable either due to low convergence speed which may allow disturbances to accumulate, the results give flexibility in meeting versatile requirements in practical PCO applications.

Acknowledgment

The authors would like to thank Francesco Ferrante for discussions and feedback which greatly strengthened the paper.

Appendix A. Lemma 5

Lemma 5. For N PCOs interacting on an undirected chain, if the PRF $F_j(x_j)$ satisfies [Assumption 3](#) and $l_j \in (0, 1)$ holds for all $j \in \mathcal{V}$, then L in (9) cannot be retained at any nonzero value along a complete solution ϕ .

Proof. We use proof of contradiction. Since $L \in [0, N\pi]$ holds, we suppose that for some $r \in (0, N\pi]$, L is retained at r along a complete solution ϕ . From [Lemma 4](#), to keep L at r , we must have

$$\Delta_{i-1}^+ = \Delta_{i-1} - \delta_{i-1}, \quad \Delta_{i-2}^+ = \Delta_{i-2} + \delta_{i-1} \quad (25)$$

or

$$\Delta_i^+ = \Delta_i - \delta_{i+1}, \quad \Delta_{i+1}^+ = \Delta_{i+1} + \delta_{i+1} \quad (26)$$

if the left-neighbor oscillator $i-1$ or right-neighbor oscillator $i+1$ exists when oscillator i fires, respectively. Next we show that Δ_N will exceed π , which contradicts the constraint $0 \leq \Delta_i \leq \pi$ for $i \in \mathcal{V}$.

Given $1 \notin \mathcal{N}_i^{\text{out}}$ and $N \notin \mathcal{N}_i^{\text{out}}$ for $i = 3, 4, \dots, N-2$, both $x_1^+ = x_1$ and $x_N^+ = x_N$ hold when oscillators $3, 4, \dots, N-2$ fire, which leads to $\Delta_N^+ = \Delta_N$. Similarly, $N \notin \mathcal{N}_1^{\text{out}}$ (resp. $1 \notin \mathcal{N}_N^{\text{out}}$) implies $x_N^+ = x_N$ (resp. $x_1^+ = x_1$) when oscillator 1 (resp. N) fires, which leads to $\Delta_N^+ = \Delta_N$ when oscillator 1 or N fires.

So we focus on the evolution of Δ_N when oscillators 2 and $N-1$ fire. According to [Lemma 6](#) in [Appendix B](#), neither oscillator

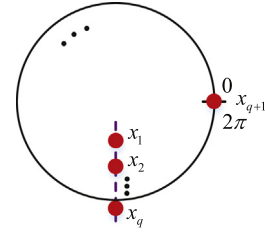


Fig. 8. Illustration of a set of $q \geq 2$ neighboring oscillators being synchronized.

2 nor oscillator $N-1$ will stop firing. Without loss of generality, we assume that oscillator 2 fires at time (t_2^*, k_2^*) . From (25) we have $\Delta_N^+ = \Delta_N + \delta_1$. Similarly, from (26) we have $\Delta_N^+ = \Delta_N + \delta_N$ when oscillator $N-1$ fires. Since δ_1 and δ_N are nonnegative, we have $\Delta_N^+ \geq \Delta_N$. To prove that Δ_N will surpass π , we need to show that at least one of the following statements is true:

- (1) $\delta_1 = 0$ cannot always hold when oscillator 2 fires;
- (2) $\delta_N = 0$ cannot always hold when oscillator $N-1$ fires.

Proof of statement (1): Given $l_1 \in (0, 1)$, according to (6) and (11), $\delta_1 = 0$ holds if and only if $x_1 = 0$ or $x_1 = 2\pi$ holds, which means that oscillators 1 and 2 are synchronized when oscillator 2 fires. So we need to show that oscillators 1 and 2 cannot always be synchronized when oscillator 2 fires. More generally, we assume that there is a set of $q \geq 2$ oscillators $1, 2, \dots, q$ being synchronized and having phases different from oscillator $q+1$. According to [Lemma 6](#) in [Appendix B](#), oscillator $q+1$ will not stop firing in this situation. We assume that oscillator $q+1$ fires at time (t_{q+1}^*, k_{q+1}^*) , and $x_1 = \dots = x_q \in [\pi, 2\pi)$ holds when oscillator $q+1$ fires, as illustrated in [Fig. 8](#). Note that the case of $x_1 = \dots = x_q \in (0, \pi]$ can be proved by following the same line of reasoning. Given $0 < l_q < 1$, from (6) and (11) we have $0 < \delta_q < 2\pi - x_q$. Since oscillator q is the left-neighbor of oscillator $q+1$, according to (25), when oscillator $q+1$ fires we have $\Delta_q^+ = \Delta_q - \delta_q = 2\pi - x_q - \delta_q > 0$ and $\Delta_{q-1}^+ = \Delta_{q-1} + \delta_q = 0 + \delta_q > 0$. So oscillator q escapes from the set of synchronized oscillators due to $\Delta_{q-1}^+ > 0$ and will fire next. Similarly, when oscillator q fires, the left-neighbor oscillator $q-1$ will escape from the set of synchronized oscillators and fire next. Iterating this argument, when oscillator 3 fires, the left-neighbor oscillator 2 will escape from the set of synchronized oscillators and fire next. So we have $x_2 \neq x_1$, i.e., oscillators 1 and 2 are not synchronized when oscillator 2 fires. Therefore, $\delta_1 = 0$ cannot always hold when oscillator 2 fires.

Similarly, we can prove statement (2), i.e., δ_N cannot always be 0 when oscillator $N-1$ fires, and thus Δ_N will keep increasing. Since δ_1 and δ_N will not converge to 0 unless synchronization is achieved, Δ_N will surpass π , which contradicts the constraint $0 \leq \Delta_i \leq \pi$ for $i \in \mathcal{V}$. Therefore, L cannot be retained at any nonzero value along a complete solution ϕ . ■

Appendix B. Lemma 6

Lemma 6. For N PCOs interacting on an undirected chain, if the PRF $F_j(x_j)$ satisfies [Assumption 3](#) and $l_j \in (0, 1)$ holds for all $j \in \mathcal{V}$, we have the following results:

- (1) Neither oscillator 2 nor oscillator $N-1$ will stop firing;
- (2) Oscillator $q+1$ will not stop firing if oscillators $1, \dots, q$ ($2 \leq q \leq N-1$) have been synchronized and oscillator $q+1$ is not synchronized with these q oscillators. Similarly, oscillator $N-q$ will not stop firing if oscillators $N-q+1, \dots, N$ have been synchronized and oscillator $N-q$ is not synchronized with these q oscillators.

Proof. We first use proof of contradiction to prove statement (1). Suppose that oscillator 2 stops firing after time instant (t'_2, k'_2) , then x_2 will stay in $[0, \pi]$. This is because if $x_2 \in (\pi, 2\pi)$ holds, it will evolve continuously to 2π and fire, and receiving pulses from other oscillators can only expedite this process under the PRFs in Assumption 3. Since oscillator 2 only receives pulses from oscillators 1 and 3, without loss of generality, we suppose at time (t'_1, k'_1) that oscillator 1 fires and resets its phase to 0. Note that oscillator 1 will fire at a period of $T_1 = 2\pi/\omega$ since its only neighbor oscillator 2 stops firing. After receiving the pulse, oscillator 2 updates its phase to $x_2^+ = x_2 + I_2 F_2^{(1)}(x_2) \in [0, \pi]$. If oscillator 2 does not receive any other pulse before its phase surpasses π , it will fire, which contradicts the assumption. So we suppose that oscillator 3 fires at time (t'_3, k'_3) before x_2 surpasses π , which implies $t'_3 - t'_1 \leq \pi/\omega$. Since the time it takes for phase evolving from 0 to π is at least π/ω and after reaching π oscillator 3 will not fire immediately even if it receives a pulse under given PRFs and coupling strengths, the length of oscillator 3's firing period T_3 satisfies $T_3 > \pi/\omega$. There are two cases in this situation, $t'_1 = t'_3$ and $t'_1 < t'_3$, respectively:

Case 1: If $t'_1 = t'_3$ holds, then the length of time interval for oscillator 2 receiving the next pulse after $(t'_3, k'_3 + 1)$ is greater than π/ω . Since $x_2(t'_3, k'_3 + 1) \geq 0$ holds, x_2 will be greater than π when receiving the next pulse. So oscillator 2 will fire again, which contradicts the assumption.

Case 2: If $t'_1 < t'_3$ holds, then we have $x_2(t'_3, k'_3 + 1) > 0$ due to $x_2(t'_3, k'_3) = x_2(t'_1, k'_1 + 1) + \omega(t'_3 - t'_1) > 0$ under given PRFs and coupling strengths. Since $t'_3 - t'_1 \leq \pi/\omega$ holds, after time interval $[\pi - x_2(t'_3, k'_3 + 1)]/\omega$ which is less than π/ω , we have $x_1 < 2\pi$, $x_3 < \pi$, and $x_2 = \pi$. So x_2 will be greater than π when receiving the next pulse, and thus oscillator 2 will fire again, which contradicts the assumption.

Therefore, oscillator 2 will not stop firing. Similarly, we can prove that oscillator $N - 1$ will not stop firing either.

Next we prove statement (2). Suppose that oscillator $q + 1$ stops firing after time (t'_{q+1}, k'_{q+1}) . Since oscillators 1, ..., q will not receive any pulses from other oscillators, they will remain synchronized and oscillator q will fire with a period of $T_q = 2\pi/\omega$. The same as statement (1), the length of oscillator $q + 2$'s firing period T_{q+2} satisfies $T_{q+2} > \pi/\omega$ and oscillator $q + 1$ will not stop firing if oscillator $q + 1$ has a phase different from synchronized oscillators 1, ..., q . Similarly, we can prove that oscillator $N - q$ will not stop firing either if oscillator $N - q$ has a phase different from synchronized oscillators $N - q + 1, \dots, N$. ■

References

- Achuthan, S., & Canavier, C. C. (2009). Phase-resetting curves determine synchronization, phase locking, and clustering in networks of neural oscillators. *Journal of Neuroscience*, 29(16), 5218–5233.
- Acker, C. D., Kopell, N., & White, J. A. (2003). Synchronization of strongly coupled excitatory neurons: relating network behavior to biophysics. *Journal of Computational Neuroscience*, 15(1), 71–90.
- An, Z., Zhu, H., Li, X., Xu, C., Xu, Y., & Li, X. (2011). Nonidentical linear pulse-coupled oscillators model with application to time synchronization in wireless sensor networks. *IEEE Transactions on Industrial Electronics*, 58(6), 2205–2215.
- Canavier, C. C., & Achuthan, S. (2010). Pulse coupled oscillators and the phase resetting curve. *Mathematical Biosciences*, 226(2), 77–96.
- Canavier, C. C., & Tiktadi-Hamburyan, R. A. (2017). Globally attracting synchrony in a network of oscillators with all-to-all inhibitory pulse coupling. *Physical Review E*, 95(3), 032215.
- Chen, C. C. (1994). Threshold effects on synchronization of pulse-coupled oscillators. *Physical Review E*, 49, 2668–2672.
- Dror, R., Canavier, C. C., Butera, R. J., Clark, J. W., & Byrne, J. H. (1999). A mathematical criterion based on phase response curves for stability in a ring of coupled oscillators. *Biological Cybernetics*, 80(1), 11–23.
- Ermentrout, B. (1996). Type I membranes, phase resetting curves, and synchrony. *Neural Computation*, 8(5), 979–1001.
- Ernst, U., Pawelzik, K., & Geisel, T. (1995). Synchronization induced by temporal delays in pulse-coupled oscillators. *Physical Review Letters*, 74, 1570–1573.
- Ferrante, F., & Wang, Y. Q. (2017). Robust almost global splay state stabilization of pulse coupled oscillators. *IEEE Transactions on Automatic Control*, 62(6), 3083–3090.
- Furukawa, T., Durrant-Whyte, H. F., Dissanayake, G., & Sukkarieh, S. (2003). The coordination of multiple uavs for engaging multiple targets in a time-optimal manner. In *2003 IEEE/RSJ international conference on intelligent robots and systems: Vol. 1* (pp. 36–41). IEEE.
- Gao, H., & Wang, Y. Q. (2018). A pulse based integrated communication and control design for decentralized collective motion coordination. *IEEE Transactions on Automatic Control*, 63(6), 1858–1864.
- Goebel, R., Sanfelice, R. G., & Teel, A. R. (2012). *Hybrid dynamical systems: modeling, stability, and robustness*. Princeton: Princeton University Press.
- Goel, P., & Ermentrout, B. (2002). Synchrony, stability, and firing patterns in pulse-coupled oscillators. *Physica D*, 163(3), 191–216.
- Golubitsky, M., & Stewart, I. (2003). *The symmetry perspective: from equilibrium to chaos in phase space and physical space: Vol. 200*. Springer Science & Business Media.
- Hansel, D., Mato, G., & Meunier, C. (1995). Synchrony in excitatory neural networks. *Neural Computation*, 7(2), 307–337.
- Hong, Y. W., & Scaglione, A. (2005). A scalable synchronization protocol for large scale sensor networks and its applications. *IEEE Journal on Selected Areas in Communications*, 23, 1085–1099.
- Hu, A., & Servetto, S. D. (2006). On the scalability of cooperative time synchronization in pulse-connected networks. *IEEE Transaction on Information Theory*, 52, 2725–2748.
- Izhikevich, E. (2007). *Dynamical systems in neuroscience: the geometry of excitability and bursting* (pp. 438–448). London: MIT Press.
- Kannapan, D., & Bullo, F. (2016). Synchronization in pulse-coupled oscillators with delayed excitatory/inhibitory coupling. *SIAM Journal on Control and Optimization*, 54(4), 1872–1894.
- Kirk, V., & Stone, E. (1997). Effect of a refractory period on the entrainment of pulse-coupled integrate-and-fire oscillators. *Physics Letters A*, 21, 70–76.
- Klinglmayr, J., & Bettstetter, C. (2010). Synchronization of inhibitory pulse-coupled oscillators in delayed random and line networks. In *Proc. 3rd IEEE int. symp. appl. sci. biomed. commun. technol.* (pp. 1–5).
- Klinglmayr, J., & Bettstetter, C. (2012). Self-organizing synchronization with inhibitory-coupled oscillators: convergence and robustness. *ACM Transactions on Autonomous Adapting System*, 7(3), 30.
- Klinglmayr, J., Bettstetter, C., Timme, M., & Kirst, C. (2017). Convergence of self-organizing pulse-coupled oscillator synchronization in dynamic networks. *IEEE Transactions on Automatic Control*, 62(4), 1606–1619.
- Klinglmayr, J., Kirst, C., Bettstetter, C., & Timme, M. (2012). Guaranteeing global synchronization in networks with stochastic interactions. *New Journal of Physics*, 14(7), 073031.
- Konishi, K., & Kokame, H. (2008). Synchronization of pulse-coupled oscillators with a refractory period and frequency distribution for a wireless sensor network. *Chaos*, 18, 033132.
- LaMar, M. D., & Smith, G. D. (2010). Effect of node-degree correlation on synchronization of identical pulse-coupled oscillators. *Physical Review E*, 81(4), 046206.
- Lyu, Hanbaek. (2015). Hanbaek lyu synchronization of finite-state pulse-coupled oscillators. *Physica D: Nonlinear Phenomena*, 303, 28–38.
- Lyu, Hanbaek (2018). Hanbaek lyu global synchronization of pulse-coupled oscillators on trees. *SIAM Journal on Applied Dynamical Systems*, 17(2), 1521–1559.
- Mathar, R., & Mattfeldt, J. (1996). Pulse-coupled decentral synchronization. *SIAM Journal of Applied Mathematics*, 56, 1094–1106.
- Mauroy, A. (2011). On the dichotomic collective behaviors of large populations of pulse-coupled firing oscillators (Ph.D. thesis), Liège, Belgium: Université de Liège.
- Memmesheimer, R. M., & Timme, M. (2010). Stable and unstable periodic orbits in complex networks of spiking neurons with delays. *Dynamical Systems*, 28(4), 1555–1588.
- Mirollo, R., & Strogatz, S. (1990). Synchronization of pulse-coupled biological oscillators. *SIAM Journal of Applied Mathematics*, 50, 1645–1662.
- Nishimura, J., & Friedman, E. J. (2011). Robust convergence in pulse-coupled oscillators with delays. *Physical Review Letters*, 106(19), 194101.
- Núñez, F., Wang, Y. Q., & Doyle III, F. J. (2015a). Synchronization of pulse-coupled oscillators on (strongly) connected graphs. *IEEE Transactions on Automatic Control*, 60(6), 1710–1715.
- Núñez, F., Wang, Y. Q., & Doyle III, F. J. (2015b). Global synchronization of pulse-coupled oscillators interacting on cycle graphs. *Automatica*, 52, 202–209.
- Núñez, F., Wang, Y. Q., Teel, A. R., & Doyle III, F. J. (2016). Synchronization of pulse-coupled oscillators to a global pacemaker. *Systems & Control Letters*, 88, 75–80.
- Pagliari, R., & Scaglione, A. (2011). Scalable network synchronization with pulse-coupled oscillators. *IEEE Transactions on Mobile Computing*, 10, 392–405.
- Paley, D. A., Leonard, N. E., Sepulchre, R., Grunbaum, D., & Parrish, J. K. (2007). Oscillator models and collective motion. *IEEE Control Systems*, 27(4), 89–105.

- Peskin, C. S. (1975). *Mathematical aspects of heart physiology*. Courant Institute of Mathematical Science, New York University.
- Proskurnikov, A. V., & Cao, M. (2015). Event-based synchronization in biology: Dynamics of pulse coupled oscillators. In *Proceedings of the first intern. conf. on event-based control, communication and signal processing*.
- Proskurnikov, A. V., & Cao, M. (2017). Synchronization of pulse-coupled oscillators and clocks under minimal connectivity assumptions. *IEEE Transactions on Automatic Control*, 62(11), 5873–5879.
- Rhouma, M. B. H., & Frigui, H. (2001). Self-organization of pulse-coupled oscillators with application to clustering. *IEEE Transactions on Pattern Analysis and Machine Intelligence*, 23(2), 180–195.
- Rockafellar, R. T., & Wets, R. J.-B. (2009). *Variational analysis: Vol. 317*. Princeton: Springer Science & Business Media.
- Simeone, O., Spagnolini, U., Bar-Ness, Y., & Strogatz, S. (2008). Distributed synchronization in wireless networks. *IEEE Signal Processing Magazine*, 25, 81–97.
- Timme, M., & Wolf, F. (2008). The simplest problem in the collective dynamics of neural networks: is synchrony stable? *Nonlinearity*, 21(7), 1579.
- Timme, M., Wolf, F., & Geisel, T. (2002). Coexistence of regular and irregular dynamics in complex networks of pulse-coupled oscillators. *Physical Review Letters*, 89(25), 258701.
- Valbuena, L., Cruz, P., Figueroa, R., Sorrentino, F., & Fierro, R. (2014). Stable formation of groups of robots via synchronization. In *2014 IEEE/RSJ international conference on intelligent robots and systems* (pp. 376–381). IEEE.
- Vreeswijk, C. V., Abbott, L. F., & Ermentrout, G. B. (1994). When inhibition not excitation synchronizes neural firing. *Journal of Computational Neuroscience*, 1, 313–321.
- Wang, Y. Q., & Doyle III, F. J. (2012). Optimal phase response functions for fast pulse-coupled synchronization in wireless sensor networks. *IEEE Transactions on Signal Processing*, 60(10), 5583–5588.
- Wang, Y. Q., Núñez, F., & Doyle III, F. J. (2012). Energy-efficient pulse-coupled synchronization strategy design for wireless sensor networks through reduced idle listening. *IEEE Transactions on Signal Processing*, 60, 5293–5306.
- Wang, Y. Q., Núñez, F., & Doyle III, F. J. (2013a). Statistical analysis of the pulse-coupled synchronization strategy for wireless sensor networks. *IEEE Transactions on Signal Processing*, 61, 5193–5204.

Wang, Y. Q., Núñez, F., & Doyle III, F. J. (2013b). Increasing sync rate of pulse-coupled oscillators via phase response function design: theory and application to wireless networks. *IEEE Transactions on Control System Technologies*, 21, 1455–1462.

Yun, S., Ha, J., & Kwak, B. J. (2015). Robustness of biologically inspired pulse-coupled synchronization against static attacks. In *Proc. IEEE global commun. conf* (pp. 1–6). IEEE.



Huan Gao was born in Shandong, China. He received the B.S. degree in automation and M.Sc. degree in control theory and control engineering from Northwestern Polytechnical University, Xi'an, Shaanxi, China, in 2011 and 2015, respectively. Currently, he is working toward the Ph.D. degree at Clemson University. His research focuses on cooperative control and dynamics of pulse-coupled oscillators.



Yongqiang Wang was born in Shandong, China. He received the B.S. degree in electrical engineering and automation, the B.S. degree in computer science and technology from Xi'an Jiaotong University, Xi'an, Shaanxi, China, in 2004, and the M.Sc. and Ph.D. degrees in control science and engineering from Tsinghua University, Beijing, China, in 2009. From 2007 to 2008, he was with the University of Duisburg-Essen, Germany, as a Visiting Student. He was a Project Scientist with the University of California at Santa Barbara, Santa Barbara. He is currently an Assistant Professor with the Department of Electrical and Computer Engineering, Clemson University. His research interests are cooperative and networked control, synchronization of wireless sensor networks, systems modeling and analysis of biochemical oscillator networks, and model-based fault diagnosis.

He was a recipient of the 2008 Young Author Prize from the IFAC Japan Foundation for a paper presented at the 17th IFAC World Congress in Seoul.